1. Benaissa Tahar [1], 2. Mahi Djillali[1], 3. Halbaoui Khaled[2]

Amar TELIDJI University of Laghouat, Algeria, Department of Electrical Engineering, Faculty of Science. (1)
Nuclear Research Centre of Brine CRNB, Power Electronics Laboratory (2)
ORCID: 1. 0000-0002-7795-1811; 2. 0000-0002-0396-2139; 3. 0000-0002-7591-4750

Maximum Power Point Tracking under simplified sliding mode control based DC-DC boost converters

Abstract. In this paper, a design of a simplified sliding mode controller (SMC) for Boost DC-DC converter in continuous conduction mode of operation is presented by defining a simplified formulation for sliding surface. The robustness and stability of the proposed controller are investigated to environment changes. Simulation results show that SMC provides good performance under the climatic changes in term of stability and robustness to irradiance and temperature variations. The proposed converter is a cascaded boost converters under Sliding Mode Control (SMC). The operation of the proposed control of dc–dc converter topology has been verified through simulation using Simulink and its performance has been shown to be satisfactory.

Streszczenie. W artykule przedstawiono projekt uproszczonego sterownika trybu ślizgowego (SMC) dla przekształtnika Boost DC-DC w trybie pracy ciągłej przewodzenia poprzez zdefiniowanie uproszczonego sformułowania dla powierzchni ślizgowej. Odporność i stabilność proponowanego kontrolera są badane pod kątem zmian środowiskowych. Wyniki symulacji pokazują, że SMC zapewnia dobrą wydajność przy zmianach klimatycznych pod względem stabilności i odporności na napromienienie i zmiany temperatury. Proponowany konwerter to kaskadowe przetwornice podwyższające w trybie sterowania przesuwnego (SMC). Działanie proponowanego sterowania topologią przekształtnika DC – DC zostało sprawdzone w drodze symulacji z wykorzystaniem Simulink i jego działanie okazało się zadowalające.(Śledzenie maksymalnego punktu mocy w przypadku konwerterów podwyższających DC-DC z uproszczonym sterowaniem przesuwnym

Keywords: Boost converters, maximum power point tracking (MPPT); photovoltaic systems, sliding mode control (SMC).
Słowa kluczowe: przekształtnik Boos DC-DC, tryb ślizgowy, maksymalny punkt mocy.

Introduction

The photovoltaic energy that is one of the important sources of renewable energy which presents a denouement to our problems of production of energy In addition, this energy seems the most promising, non-polluting and inexhaustible [1]. Nevertheless, the I-V characteristic of the GPV depends on the level of insolation and the temperature of the cell as well as the aging of the assembly. Moreover, its operating point of the GPV depends directly on the load it supplies. In order to extract at each instant the maximum power available at the terminals of the GPV, we introduce an adaptation stage between the generator and the load to couple the two elements as perfectly as possible [1], [2]. The problem of the perfect coupling between a photovoltaic generator and a continuous type load is not yet resolved. One of the technological locks that exist in this type of coupling is the problem of transferring the maximum power of the photovoltaic generator (PVG) to the load which often suffers from poor adaptation. The resulting operating point is sometimes very far from the maximum power point (MPP).

In order to ensure that the maximum power is permanently generated, the maximum power point is determined using a maximum power point tracking technique (MPPT) [3], [5]. In this context, several studies have focused on photovoltaic systems, Several MPPT techniques have been developed for PVG system. Hill-Climbing, Perturbing and Observing (P&O) and Conductance Increment were widely used in MPPT controller [6]. Other controls have been developed such as measuring a short circuit current fraction (FCC) or measuring an open circuit voltage fraction (FCO). There are also so-called intelligent commands that are based on neural network and fuzzy logic [7], [8].

For a while now, the sliding mode control (SMC) method has been developed as a general control method to be applied to a large set of system types, including non-linear systems, multiple input/output systems, discrete time models, large scale and infinite dimensional systems [9, 10].

It has been widely accepted for some time that sliding mode control is very adequate for the control of switched mode converters [11] - [14]. It can be set up as a control strategy with a variable structure based on feedback and high-frequency switching control. The SMC has numerous features such as high stability, insensitivity to changes in system parameters, disturbances and load variations [15] and generally, it is simple to implement depending on the sliding surface. The two main steps in the design of an SMC are the design of a stable sliding surface and the optimal design of a control low, which allows in a short time the operating points to reach a predetermined area [16]. The sliding mode controller needs to maintain a constant gain in order to achieve a robust and finite convergence of the sliding boundary over time.

The objective of the SMC application is therefore to provide the MPPT system with the necessary control support for stability with robustness against parameter uncertainties and fast dynamic responses under rapidly changing environmental conditions, since conventional MPPT controllers (digital or analog) cannot meet these requirements without continuous adjustment of the controller parameters and a complex controller architecture [17, 18].

In this paper, a cascaded boost converter under sliding mode control has been applied for the search and tracking of the maximum power point for PV arrays. It will be used as a solution for the purpose of adapting the electrical energy that comes from the Photovoltaic panels, in order to be able to supply loads.

System Overview

In the present investigation, the proposed conversion system is described by Fig 1. It consists of a PV array, two DC-DC boost converter, an MPPT command under sliding mode control (SMC). However, the analysis reported in the present document can be generalized to other DC/DC converters topologies. The following section describes briefly the different parts of the system.
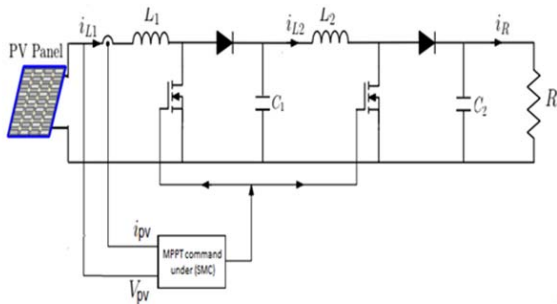
Fig. 1. Schematic diagram of the proposed PV system with cascaded boost converter.

Simulations are performed on a typical boost converter of parameters shown in Table I

Table I · The boost converter parameters

Parameter	Variable	Value
Inductor	L_1	200 µH
Capacitor	C_1	10 µF
Inductor	L_2	2 mH
Capacitor	C_2	10 µF
Resistor	R	800Ω

Photovoltaic generator model

As shown in Figure 2, the PV cells are modeled using the single-diode model. The model includes a photocurrent source Iph, a parallel diode Dp and two resistors for losses, a parallel resistor Rp and a series resistor Rs. The technical characteristics of the solar cells of this model are given by the manufacturers (data sheets).
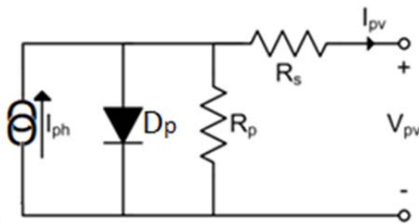
Fig. 2. Single diode circuit model for a photovoltaic cell.

The photocurrent source and resulting power generated by the PV cells are directly influenced by light and temperature intensity on the PV panel. The power-voltage curves for the PV cell models for different insolation and temperature intensity are shown in Figure 3.

Full-order switched model

In this work, a cascaded two-stage boost converter (Figure1) is synthesized using a single sliding surface by sensing the input voltage and current of the first converter. Both cascaded converters will be driven by the same control signal.

By applying Kirchhoff's laws of voltage and current to the circuit in Figure 1, and assuming that both converters operate in continuous conduction mode, the two-cascaded converters can be represented by the following set of differential equations.

(1) $\qquad \frac{di_{L_1}}{dt} = \frac{V_{pv}}{L_1} - \frac{v_{c1}}{L_1}(1-u)$

(2) $\qquad \frac{di_{L_2}}{dt} = \frac{v_{c1}}{L_2} - \frac{v_{c2}}{L_2}(1-u)$

(3) $\qquad \frac{dv_{c_1}}{dt} = \frac{i_{L1}}{C_1}(1-u) - \frac{i_{L2}}{C_1}$

(4) $\qquad \frac{dv_{c_2}}{dt} = \frac{i_{L2}}{C_2}(1-u) - \frac{v_{c2}}{RC_2}$

where u is the discontinuous control variable for the two converter stages (u = 1 when the converter switchs are closed and u = 0 when the switchs are open.) and i_{L1}, v_{C1}, i_{L2}, v_{C2} are the instantaneous input currents and output voltages, of the two boost stage respectively

a)
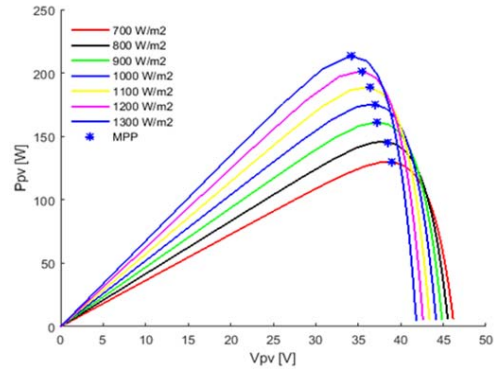
b)
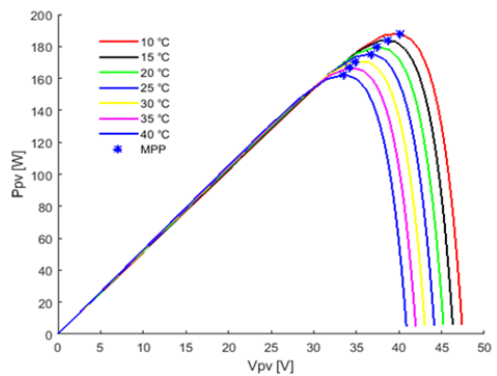
Fig. 3. PV cell characteristics under different (a) Irradiance   level (b) temperature level

The Proposed Sliding Mode Control Approach

The Boost converter is widely employed when the output voltage must be equal or higher than the input one. In this document, the boost converter is used to adapt the output voltage so the load can better benefit from the maximum power delivered by the PV. The sliding mode controller is used to regulate the output voltage of the boost converter. This controller limits the operation of the system to the sliding switch surface. The control of the sliding mode is done in two steps. In the first step, an equilibrium surface is chosen and then in the second step, a discontinuous control law will be determined. As it is known, the non-linear relationship between PV current and voltage produces a non-linear relationship between PV power and voltage, which has a maximum as shown in Figure 3. In such a maximum, i.e. PPM, the derivative of power versus voltage is equal to zero as shown in equation (5). In the present document the sliding surface is taken based on equation (5).

(5) $\qquad S = \frac{dP}{dV}$

Now, by designing the above surface, we should obtain for the boost converter a control law that forces the system to move on the sliding mode surface in a finite time. The control signal calculation is expressed by the following relation:

(6) $\qquad U = Ueq + Un$

Where Ueq is the equivalent control and Un is the switching control term. Ueq is obtained from the invariance condition and is given as below:

$$S = 0 \text{ and } \dot{S} = 0 \iff U = U_{eq}$$

For the converter the derivative of the sliding surface (Eq. 5) is:

(7) $$\dot{S} = \frac{d}{dt}\left[\frac{dP}{dV}\right] = \frac{d}{dt}\left[\frac{d(VI)}{dV}\right]$$

(8) $$\dot{S} = 2\frac{dI}{dt} + V\frac{dI}{dtdv}$$

(9) $$\dot{S} = \left[2 + V\frac{dI}{dv}\right]\frac{dI}{dt} = K\frac{dI}{dt}$$

Where:

(10) $$K = \left[2 + V\frac{dI}{dv}\right]$$

Substituting Eq. (1) into Eq. (8) results in:

(11) $$\dot{S} = K\left[\frac{V_{pv}}{L_1} - \frac{v_{c1}}{L_1}(1-u)\right]$$

By imposing the invariance conditions $S = 0$ and $\dot{S} = 0$ we obtain:

(12) $$\dot{S} = 0 \rightarrow \frac{V_{pv}}{L_1} - \frac{v_{c1}}{L_1}(1-u) = 0$$

Considering Eq. (11) the equivalent control-input is obtained as:

(13) $$u_{eq}(t) = 1 - \frac{V_{pv}}{V_{c1}}$$

In order to ensure convergence to the trajectory of the sliding surface, Un is chosen so that the Lyapunov stability criterion ($dS *S < 0$) is respected.

(14) $$u_n(t) = \frac{V_{pv}}{V_{c1}} - A$$

where A is the control signal which is calculated according to Lyapunov's stability criteria.

Substituting Eq. (13) and Eq. (14) into Eq. (6) results in the control law as:

(15) $$u(t) = 1 - A$$

In order to demonstrate stability, the candidate Lyapunov function is adopted:

(16) $$V = \frac{1}{2}S^2(t) \quad \text{Then: } \dot{V} = S\dot{S}(t)$$

Substituting Eq. (11) and Eq. (15) into Eq. (14) gives the following result for three different types of converters:

(17) $$\dot{V} = \frac{K}{L_1}\left[\frac{V_{pv}}{v_{c1}} - A\right]S$$

To satisfy the convergence condition given below.

(18) $$A < \frac{V_{pv}}{v_{c1}} \quad \text{if } S < 0$$

(19) $$A > \frac{V_{pv}}{v_{c1}} \quad \text{if } S > 0$$

The proposed maximum power point tracking method is presented in the flowchart Figure4. the voltage and current of the PV panel are collected directly at the output panel and thus the power Ppv(k) is obtained from the product of the collected values; the result is compared with the one obtained by the previous sampling P (k-1). If dPpv/dVpv> 0, the voltage is increased which induces a control state equal to 1 and if dPpv/dVpv<0, the voltage is reduced which translates into a 0 state for the control, i.e. the control switches between 1 and 0.

By this algorithm, the operating point of PV panel oscillates closer to the maximum power point and finally reach a steady state. The MPPT algorithm under sliding mode therefore reacts rapidly to sudden changes in operating conditions.
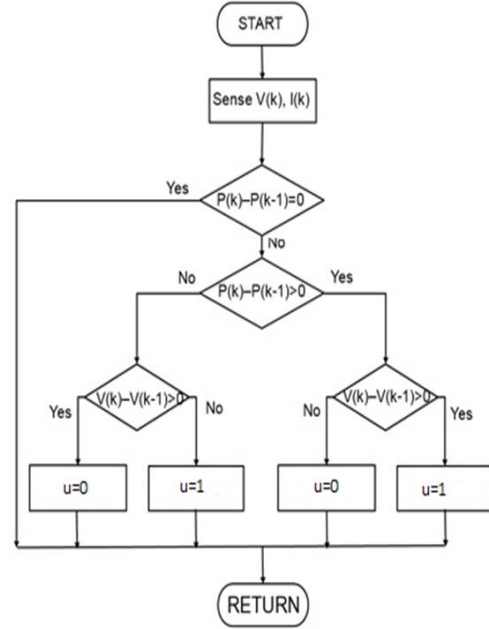
Fig.4. MPPT algorithm under sliding mode controler

Numerical simulation

With the aim of further evaluate the proposed SMC, the scheme in Figure 1 is implemented in Matlab/Simulink by considering a PV power source, two cascaded boost converter and the proposed MPPT approach under sliding mode controller. The parameters used to define the PV cell are summarized in Table II.

Table II · Parameters of the PV cell in matlab/simulink model

Parameter	Variable	Value
Current at Maximum Power	Im	4.95 A
Voltage at Maximum Power	Vm	35.2 V
Open Circuit Voltage	Voc	44.2 V
Short Circuit Voltage	Isc	5.2 A
Temperature Coefficient of Short Circuit Current	a	0.015 A/°K
Temperature Coefficient of Open Circuit Voltage	b	0.7V/°K
Internal Series Resistance	Rs	0.217Ω
Reference Solar Radiation	Sref	1000 W/m2
Reference Temperature	Tref	25°C

The response of the two cascaded boost converter connected to the PV module with an MPPT have been checked under the change of irradiance and temperature separately.

To show the robustness to irradiance, a first test was performed considering fast increase and decrease of lighting. In this case, the system is subjected to an illumination variation from 1000 W/m2 to 1300 W/m2 at time t=0.03s and then decrease to 1000 W/m2 at t=0.04s, then decrease to 700 W/m2 at time t=0.06s and finally return to 1000W/m2 at t=0.07s. The temperature is kept constant all time equal to 25°C.

The results of the simulation of the PV system using the MPPT algorithm under sliding mode for fast irradiation variation are presented in Figure4, Figure5 and Figure6.

Figure 5 shows the system trajectory due to an abrupt steps of the irradiation. At each change, the system "slides" to the new maximum power point.
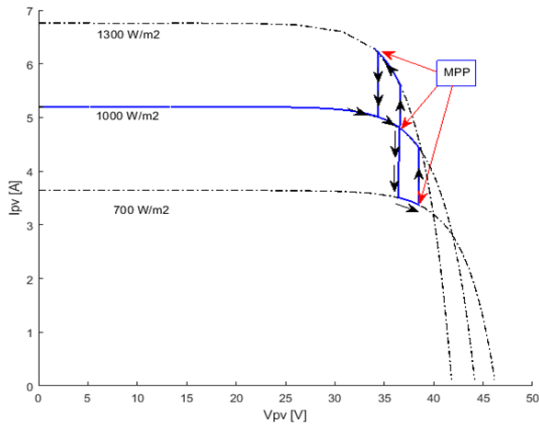
Fig.5. Convergence of sliding mode , MPPT following abrupt irradiation steps.

a)

b)
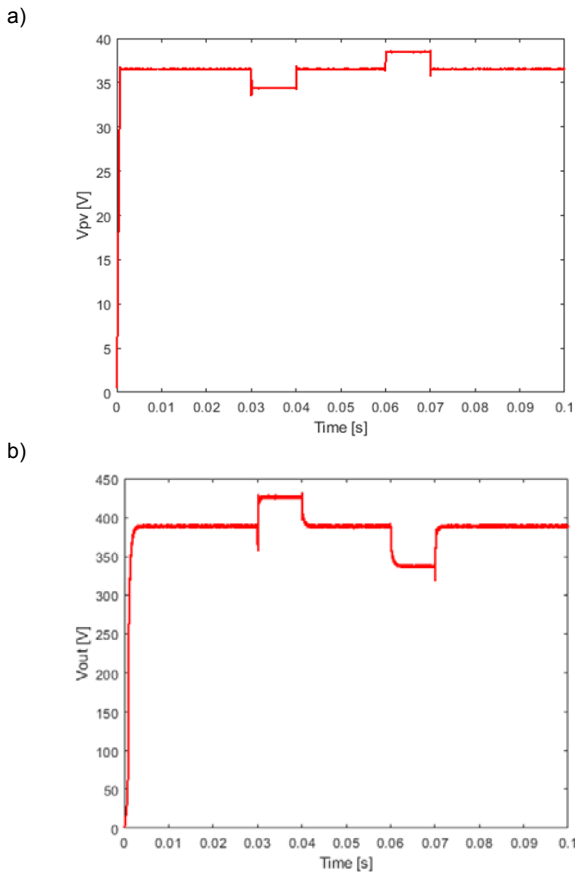
Fig.6. Input voltage and output voltage following step irradiance change a) PV voltage b) output voltage.

Figure6 and Figure7 illustrates, respectively, the PV and converter output voltage and power behaviors when facing the solar irradiation changes. It can be seen that at the instant 0.03 s the increase in insolation causes a slight decrease (-5.75%) in the PV voltage Figure6.a, however we notice a power increase Figure7.a (21.68%) due to the PV current increases (the irradiation changes affect mainly the PV output current). It can also be seen that at instant 0.06 s

the decrease in insolation causes a slight increase in the PV voltage (5.48%), however we notice a power decrease (-26%). Therefore, in both cases the operating point of the system moves away from the PPM. After a minimum convergence time, consequently, the control acts and the operating point stabilizes around the new PPM with a small oscillation.

Noting that since the load connected to the output of the boost converter is constant, any increase or decrease in the maximum power point of the PV requires an adaptation of the output voltage of the boost converter (voltage Figure6.b follows power Figure7.b the output voltage of the converter was increased by 9.23% at instant 0.03 and decreased by -13.3% at instant 0.06.) so that this load can better benefit from the maximum power provided by the PV.

a)

b)
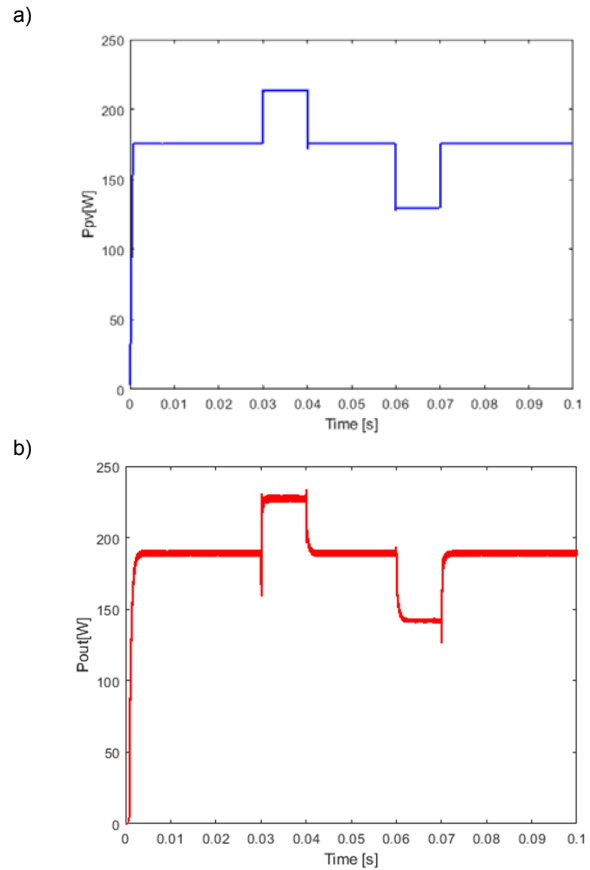
Fig.7. Input power and output power following step irradiance change, a) PV power b) output power.

As mentioned above, the second parameter influencing the photoelectric current and subsequently the resulting energy produced by the photovoltaic cells is the temperature of the PV cells.

To show the robustness to temperature variation, a test was performed considering fast increase and decrease of temperature. In this case, the system is subjected to a temperature variation from 25°C to 40°C at time t = 0.03s and then decrease to 25°C on t = 0.04s, then decrease to 10°C at time t=0.06s and finally return to 25°C at t=0.07s. The irradiation is kept constant all time equal to 1000 W/m2.

The results of the simulation of the PV system using the MPPT algorithm under sliding mode for fast temperature variation are presented in Figure8, Figure9 and Figure10.

Figure 8 shows the system trajectory due to an abrupt steps of the temperature. At each change, the system "slides" to the new maximum power points.

Figure9 and Figure10 illustrates, respectively, the PV and converter output voltage and power behaviors when facing the PV temperature changes. It can be seen that at the instant 0.03 s the increase in temperature causes a slight decrease (-8.22%) in the PV voltage Figure9.a, which induces a decrease in the power Figure10.a (-7.49%) since the PV current kept constant (the temperature changes affect mainly the PV output voltage). It can also be seen that at instant 0.06 s the decrease in temperature causes an increase in the PV voltage (8.22%), however we notice a power increase (7.27%). Therefore, in both cases very rapid small oscillations around the operating point are observed, the control acts and the operating point stabilizes around the new MPP. Consequently, the SMC proved high superiority in terms of tracking the MPP since they reach the operating point immediately regardless of any sudden change.
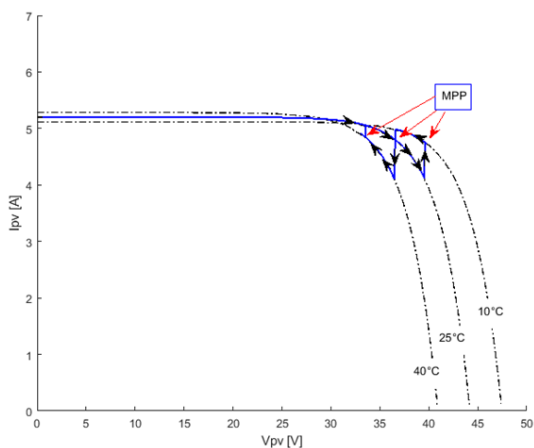
Fig.8. Convergence of sliding mode MPPT following abrupt temperature steps.

a)

b)
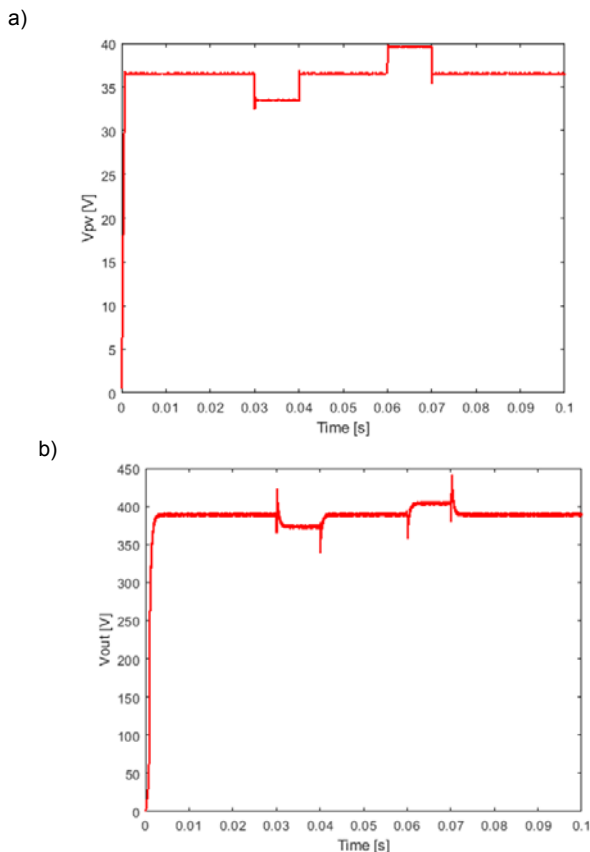
Fig.9. Input voltage and output voltage following step temperature change, a) PV voltage b) output voltage.

a)

b)
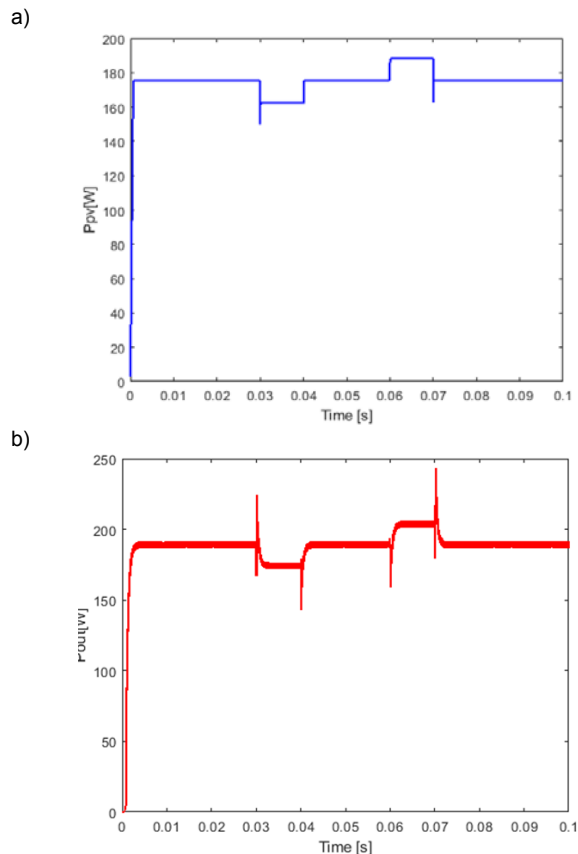
Fig.10. Input power and output power following step temperature change , a) PV power b) output power.

Noting that since the load connected to the output of the boost converter is constant, any increase or decrease in the maximum power point of the PV requires an adaptation of the output voltage of the boost converter (voltage Fig.9.b follows power Figure10.b the output voltage of the converter was decreased by -3.85% at instant 0.03 and increased by 3.59% at instant 0.06) so that this load can better benefit from the maximum power provided by the PV.

Finally, this paper describes a simplified sliding mode control based MPPT on applying a perfectly adapted switching surface. As can be seen like other SMCs, the proposed sliding mode control MPPT has two major advantages: rapid response to a change in radiation and/or temperature and stability over the entire PV curve. It is seen that the dc-dc converter with a simplified SMC has a superior transient response compared to the conventional control found in the literature.

Conclusion

In this paper, a simplified sliding mode controller was designed for DC–DC boost converter in continuous conduction mode for Maximum Power Point Tracking applications. The proposed system was simulated in Matlab/Simulink software to evaluate the proposed controller response. Special situations such as sudden changes of solar radiation and temperature have been simulated and analyzed. From the obtained results, some conclusions were made: The proposed sliding mode control MPPT has rapid response to a change in radiation and/or temperature and stability over the entire PV curve, which allows the maximum available energy to be obtained from the PV module.

The Boost converter, is able to find the PPM independently of the ambient conditions, thus, this

converter in SMC technique is more suitable to be employed as MPP Tracking, mainly in situations where the environmental conditions vary abruptly and considerably.

In addition, given the simplicity of the proposed sliding mode controller, it can be easily implemented.

Authors
T. Benaissa Email: ben_aissatahar@yahoo.fr; Djillali Mahi Email: ben_aissatahar@yahoo.fr the address of the two first authors Department of Electrical Engineering, Faculty of Science, Amar TELIDJI University of Laghouat, Algeria. Khaled Halbaoui Email: ben_aissatahar@yahoo.fr Power Electronics Laboratory, Nuclear Research Centre of Brine CRNB, Ainoussera 17200, Djelfa, Algeria.

REFERENCES

[1] Bhatnagar P., Nema R. K., "Maximum power point tracking control techniques: State of the art in photovoltaic applications Review Article", Renewable and Sustainable Energy Reviews, Vol. 23 (July 2013), pp. 224-241

[2] Dupont, E.; Koppelaar, R.; Jeanmart, H. Global available solar energy under physical and energy return on investment constraints. Appl. Energy (2020), 257, 113968.

[3] Haddou. A, Tariba.N. E, Naima. I, Bouknadel. A, El Omari. H, EL Omari. H. "Comparative study of new MPPT control approaches for a photovoltaic system". International Journal of Power Electronics and Drive System (IJPEDS) Vol. 11 (March 2020), No. 1, pp. 251~261.

[4] Manel Hlaili, Hfaiedh Mechergui, "Comparison of Different MPPT Algorithms with a Proposed One Using a Power Estimator for Grid Connected PV Systems", International Journal of Photoenergy, vol. 2016 (2016), pp. 1-10, http://dx.doi.org/10.1155/2016/1728398

[5] Mendez, E.; Ortiz, A.; Ponce, P.; Macias, I.; Balderas, D.; Molina, A. Improved MPPT Algorithm for Photovoltaic Systems Based on the Earthquake Optimization Algorithm. Energies Vol. 13 (2020), 3047.

[6] Safarin. A, Mekhilef, S. "Simulation and hardware implementation of incremental conductance MPPT with direct control method using cuk converter" IEEE transactions on industrial electronics, Vol. 58 (2010), nr 4, pp. 1154-1161.

[7] Chiu, C.-S., Ouyang, Y.-L. "Robust Maximum Power Tracking Control of Uncertain Photovoltaic Systems: A Unified T-S Fuzzy Model-Based Approach". IEEE Trans. Control Syst. Technol. Vol. 19 (2011), pp. 1516–1526.

[8] Lin, W.-M.; Hong, C.-M.; Chen, C.-H. Neural-Network-Based MPPT Control of a Stand-Alone Hybrid Power Generation System. IEEE Trans. Power Electron. Vol. 26 (2011), pp. 3571–3581.

[9] Reham Haroun Mohamed Abdelkarim "Cascaded Voltage Step-up Canonical Elements for Power Processing in PV Applications" PhD thesis, Dept. d'Enginyeria Electronica, Electrica i Automatica Universitat Rovira i Virgili, 2014

[10] A. Leon-Masich, H. Valderrama-Blavi, J. M. Bosque-Moncusí, J. Maixé-Altés and L. Martínez-Salamero, "Sliding-Mode-Control-Based Boost Converter for High-Voltage–Low-Power Applications," IEEE Transactions on Industrial Electronics, Vol. 62 (2015), nr. 1, pp. 229-237

[11] Paula. A.O.V, Carlos. A.R.P "Sliding-Mode Controller for Maximum Power Point Tracking in Grid-Connected Photovoltaic Systems" Energies Vol. 8 (2015), pp. 12363–12387; doi:10.3390/en81112318

[12] Gomathi. A, Nageswari. S, Durga D. R," Modeling and Analysis of Sliding Mode MPPT Controller for Solar Photovoltaic System" International Journal of Advanced Research in Electrical, Electronics and Instrumentation Engineering, Vol. 7 (2018), nr. 2, pp. 726-734

[13] Z. Meng, W. Shao, J. Tang and H. Zhou, "Sliding-mode control based on index control law for MPPT in photovoltaic systems," in CES Transactions on Electrical Machines and Systems, vol. 2 (September 2018), nr. 3, pp. 303-311,

doi: 10.30941/CESTEMS.2018.00038.

[14] K. Vrdoljak, N. Peric, and I. Petrovi ´ c, "Sliding mode based load- frequency control in power systems," Electric Power Systems Research, vol. 80(2010), nr. 5, pp. 514–527

[15] M. A. G. Brito, L. Galotto, Jr., L. P. Sampaio, G. A. Melo, and C. A. Canesin, "Evaluation of the main MPPT techniques for photovoltaic applications," IEEE Trans. Ind. Electron., vol. 60 (Mar 2013), nr. 3, pp. 1156–1167

[16] Mostafa R. Mustafa, Naggar H. Saad, Ahmed A. El-sattar. Tracking the maximum power point of PV array by sliding mode control method "Ain Shams Engineering Journal Vol. 11 (March 2020), nr.1, , pp. 119-131

[17] M. S. Agamy, M. H. Todorovic, A. Elasser, S. Chi, R. L. Steigerwald, J. A. Sabale, A. J. McCann, Li Zang, and F. Mueller, "An efficient partial power processing DC/DC converter for distributed PV architectures," IEEE Trans. Power Electron., Vol. 29 (Feb. 2014), nr. 12, pp. 674–686